ACS SENSORS

pubs.acs.org/acssensors

Article

# Applying CRISPR-Cas12a as a Signal Amplifier to Construct Biosensors for Non-DNA Targets in Ultralow Concentrations

Junjie Li,* Shuangshuang Yang, Chen Zuo, Ling Dai, Yongcan Guo,* and Guoming Xie*

Cite This: *ACS Sens.* 2020, 5, 970−977

Read Online

ACCESS | Metrics & More | Article Recommendations | Supporting Information

**ABSTRACT:** Efficient signal amplification is essential to construct ultrasensitive biosensors for biologically relevant species with abundant concomitant interferences. Here, we apply LbaCas12a as a signal amplifier to develop a versatile CRISPR-Cas12a platform to detect a wide range of analytes in ultralow concentrations. The platform relies on the indiscriminate single-stranded DNase activity of LbaCas12a, which recognizes single-stranded DNA intermediates generated by non-DNA targets down to femtomolar concentrations and subsequently enhances the fluorescence signal output. With the help of functional nucleotides (DNAzyme and aptamer), ultrasensitive bioassays for $Pb^{2+}$ and *Acinetobacter baumannii* have been designed with a limit of detection down to ∼0.053 nM and ∼3 CFU/mL, respectively. It also allows simultaneous detection of four microRNAs (miRNAs) at a picomolar concentration without significant interferences by other counterparts, suggesting the potential of multiplexed miRNA expression profiles analysis in high throughput. Given the versatility and generality of the CRISPR-Cas12a platform, we expect the current work to advance the application of CRISPR-Cas-based platforms in bioanalysis and provide new insights into ultrasensitive biosensor design.

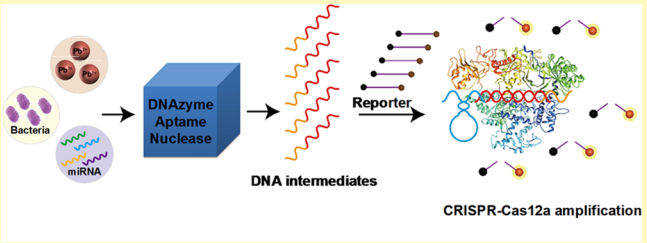


**KEYWORDS:** *CRISPR-Cas12a, signal amplifier, lead ions, Acinetobacter baumannii, microRNAs*



Ultrasensitive detection of biologically relevant species is urgently required in many aspects of daily life, including clinical diagnosis,[1] food surveillance,[2] environmental monitoring,[3] and forensic analysis.[4] However, due to rich concomitant interfering counterparts in biological matrices and inherent background signals associated with the instruments, most analytical methodologies based on large equipment cannot be used directly to determine the concentration of targets unless appropriate pretreatment processes are applied beforehand.[5] Biosensors have recently emerged as a versatile alternative to bulky instruments since they can offer rapid, cost-effective, and on-site detection of a broad range of targets,[6] which would potentially revolutionize analytical science and personalized health care to a large extent.[7] During the past decades, developing more efficient signal amplification strategies has been the focus of a copious number of biosensor design studies[8] so as to produce a meaningful signal for subsequent readout after identification of a specific analyte in low abundance. In the case of fluorescence measurement, amplification is particularly relevant in the context of biological samples as high levels of autofluorescence, light scattering, and optical aberration seriously threaten valid signal acquisition.[9] Besides, amplification of a signal can shorten data collection time, reduce requirements for high-precision setups, and thus reduce overall costs for individual measurements.

Strategies explored previously to realize efficient signal amplification can be generally divided into two categories: nanomaterials-based methods and molecular biology-based methods. Benefiting from the fruitful achievements of nanotechnology and nanoscience,[10−12] the former promises ultrasensitive in-field and even in situ detection of proteins and nucleic acids in both laboratory and clinical applications. For example, spherical nucleic acid−gold nanoparticles (SNA−AuNPs), which are composed of densely packed oligonucleotides on a AuNP core, have been introduced and extensively exploited in detection of biomolecules by Mirkin's group.[13,14] However, poor long-term stability and potential biosafety threats still remain a major challenge for most nanomaterials in general health care utilization.[15,16] In contrast, molecular biology-based signal amplification strategies, which rely on the organized reaction or interaction of biological components with or without enzymes, have shown superior power to provide safer application in both the clinic and laboratory. For instance, PCR amplification, the most popular enzyme-assisted signal amplification approach, has long been recognized as the gold standard in many applications.[17,18] However, it is impaired by the requirement of a precise primer design and a thermal cycler and the high risk of carry-over contami-

**Received:** November 21, 2019
**Accepted:** March 11, 2020
**Published:** March 11, 2020




https://dx.doi.org/10.1021/acssensors.9b02305
*ACS Sens.* 2020, 5, 970−977

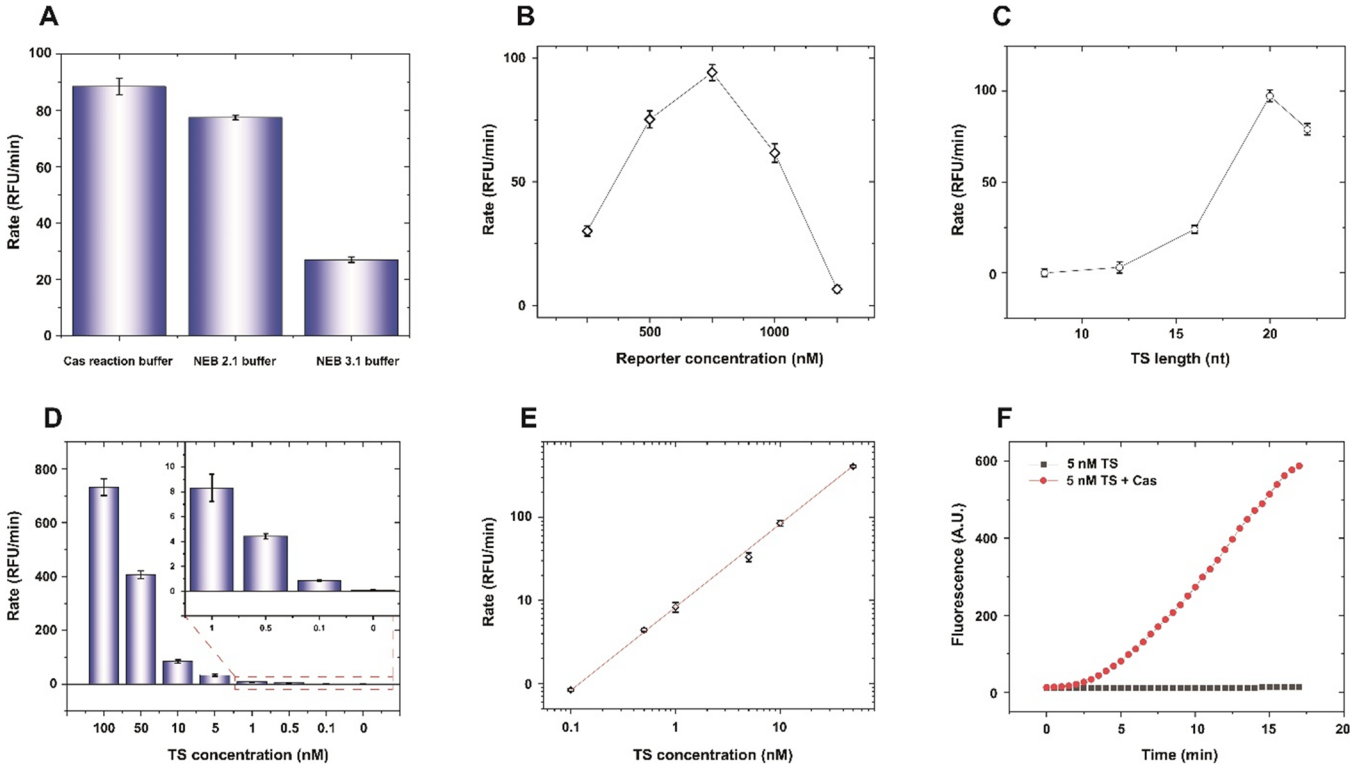


**Figure 1.** Optimization of the (A) buffer, (B) reporter concentration, and (C) target strand (TS) length to maximize the LbaCas12a cleave speed. (D) TS concentration-dependent cleave rate and (E) corresponding linear fitting. (F) Fluorescence changes of a 5 nM HEX-labeled TS and that after amplification by the CRISPR-Cas12a platform.

nation.[19] Non-enzymatic amplification schemes, mainly including the hybridization chain reaction, catalyzed hairpin assembly, and entropy-driven catalysis, have otherwise demonstrated their advantages in the field of in vitro detection due to simple, robust, low-cost features and exemption of a complicated enzyme reaction. However, despite significant advancement in those tools, the majority of them involve time-consuming multistep reactions, harsh buffer/temperature requirements, and sophisticated probe/primer designs. Therefore, new amplification schemes of high sensitivity and specificity are in critical need to circumvent the limitations associated with the current detection methodologies to afford cost-effective, reliable, and portable analytical tools to expand their practical utility.

Recently, clustered regularly interspaced short palindromic repeats (CRISPR)-associated nuclease (Cas)-based techniques have considerably expanded our toolbox in programmable and highly specific gene editing.[20,21] Through the binding of short guiding RNA molecules, known as crRNA, the CRISPR-Cas protein family can be programmed to edit specific genomic loci, thus facilitating systematic investigation and control of the target gene function.[22,23] The sequence-specific recognition capabilities of the CRISPR system have also been proved to be versatile to develop detection tools for target DNA analysis. The Zhang Lab introduced the first CRISPR-Cas-based nucleic acid detection methodology, called SHERLOCK, based on the collateral promiscuous RNase activity of Cas13a upon target RNA recognition, which showed attomolar sensitivity and single-base mismatch specificity when integrated with recombinase polymerase amplification (RPA).[24] In the upgraded version SHERLOCKv2,[25] a 3.5-fold increase in signal sensitivity was realized by combining Cas13 with Csm6, and more importantly, four-channel single reaction multiplexing is also attainable using orthogonal CRISPR enzymes. In the meantime, integration of Cas9 with strand-displacing DNA polymerase, termed Cas9Nar, can amplify the target genomic DNA fragment at a constant temperature of 37 °C with a limit of detection down to the zeptomolar level within 60 min.[26] The Doudna Lab[27] and Li et al.[28] reported the indiscriminate cleavage activities on single-stranded DNA back-to-back, resulting in two isothermal DNA detection platforms named as DETECTR and HOLMES,[29] respectively, which eliminate the need for DNA to RNA conversion required by SHERLOCK for DNA sequence detection. Unlike in other CRISPR-Cas systems, activated Cas12a by either a double-stranded or single-stranded target not only cleaves the target double-stranded DNA but also indiscriminately cleaves any nontarget single-stranded DNA (ssDNA), which is known as the collateral cleavage activity and forms the basis to develop biosensors to detect DNAs. More recently, Wang et al. found that Cas12a could also recognize the protospacer adjustment motif (PAM) sequence of UUUN rather than TTTN; thus, uracil-DNA glycosylase enzymes can be applied in a loop-mediated isothermal amplification (LAMP)-CRISPR-Cas12a system to eliminate carry-over contamination.[30] Apart from reports of Aran et al.[31] and Liang et al.,[32] the majority of CRISPR-Cas-based platforms rely on initial amplification steps via PCR reaction and have mainly been applied to targets of DNA origin.[33]

Here, we report the extension of the CRISPR-Cas12a-based fluorescence detection method to detect a variety of biologically relevant species, including heavy metal ions, bacteria, and microRNAs (miRNAs). The detection platform applies CRISPR-Cas12a as a signal amplifier to enhance the


https://dx.doi.org/10.1021/acssensors.9b02305
ACS Sens. 2020, 5, 970−977

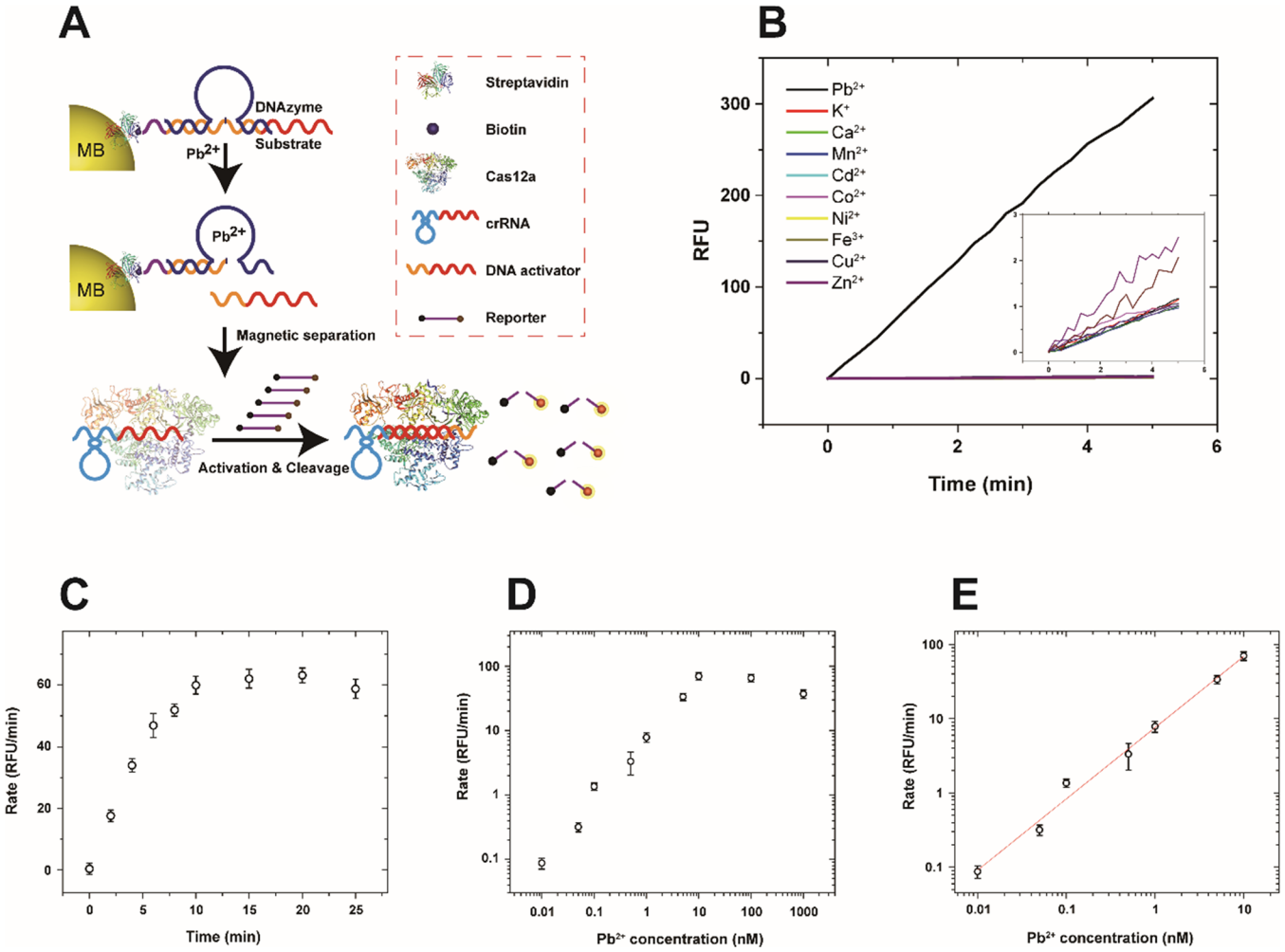


**Figure 2.** CRISPR-Cas12a-based assay for $Pb^{2+}$ detection using a $Pb^{2+}$-specific DNAzyme. (A) Schematic illustration of the design of the assay to detect $Pb^{2+}$ using DNAzyme GR-5. (B) Selectivity of the assay toward interfering metal ions at a concentration of 10 $\mu$M ($Pb^{2+}$ in 10 nM). (C) Effect of incubation time on the cleavage rates. (D) $Pb^{2+}$ concentration-dependent increase in cleavage rates. (E) Linear fitting of the cleavage rate with the concentration of $Pb^{2+}$ from 0.01 to 10 nM.

fluorescence output upon activation by ssDNA intermediates, generated only in the presence of target analytes. It allows detection of $Pb^{2+}$ at the picomolar level, *Acinetobacter baumannii* down to the single-cell level, and multiplexed miRNA analysis at the femtomolar level.

## RESULTS AND DISCUSSION

**Detection Limit of the ssDNA Target Strand (TS) under Optimized Conditions.** To extend the CRISPR-Cas12a platform to detect targets other than DNA, the basic idea is to convert non-DNA input into DNA intermediates quantitatively, which subsequently initiates the nuclease activity to cleave the reporter to produce a fluorescence signal. To approach the limit of the CRISPR-Cas12a platform to realize the highest sensitivity, we first optimized the reaction condition in room temperature to maximize the collateral cleavage activity of commercially available LbaCas12a from a Lachnospiraceae bacterium. In previous reports, cleavage of nontarget ssDNA by LbaCas12a has been frequently conducted in a commercial 1× NEB buffer[30,34] and a self-made reaction buffer containing DTT.[27,35] A comparison of the cleavage rates in three different buffers with the same target DNA concentration shows that LbaCas12a exhibited the highest activity in the Cas reaction buffer reported by Doudna et al.[27] (Figure 1A). Besides, LbaCas12a, like some other nucleases,[36] requires DTT to activate the nuclease activity, but a variation of the DTT concentration from 0.5 to 2.5 mM did not affect the cleavage speed too much (Figure S1). Based on the Michaelis–Menten equation, the apparent cleavage rates should be positively correlated with the substrate (reporter) concentrations under a constant LbaCas12a concentration. However, when a reporter concentration ranging from 0.25 to 1.25 $\mu$M was applied, the observed cleavage speed reached a maximum at 0.75 $\mu$M, and further increase of the reporter resulted in a dropped rate (Figure 1B). This perhaps issues from the calculation of cleavage speed using the growth rate of fluorescence. Meanwhile, in low reporter concentrations, intramolecular interaction dominates the quenching efficiency of reporters; intermolecular fluorescence quenching must be considered due to highly frequent molecular collisions and self-quenching mechanisms of fluorophores in high concentrations. Therefore, despite the fact that high substrate concentrations lead to fast velocity, the growth rate of fluorescence does not increase concomitantly as it is no longer proportional to the cleavage speed. To link the TS concentration directly with the fluorescence growth rate, 0.75 $\mu$M reporter was used in the


https://dx.doi.org/10.1021/acssensors.9b02305
ACS Sens. 2020, 5, 970−977

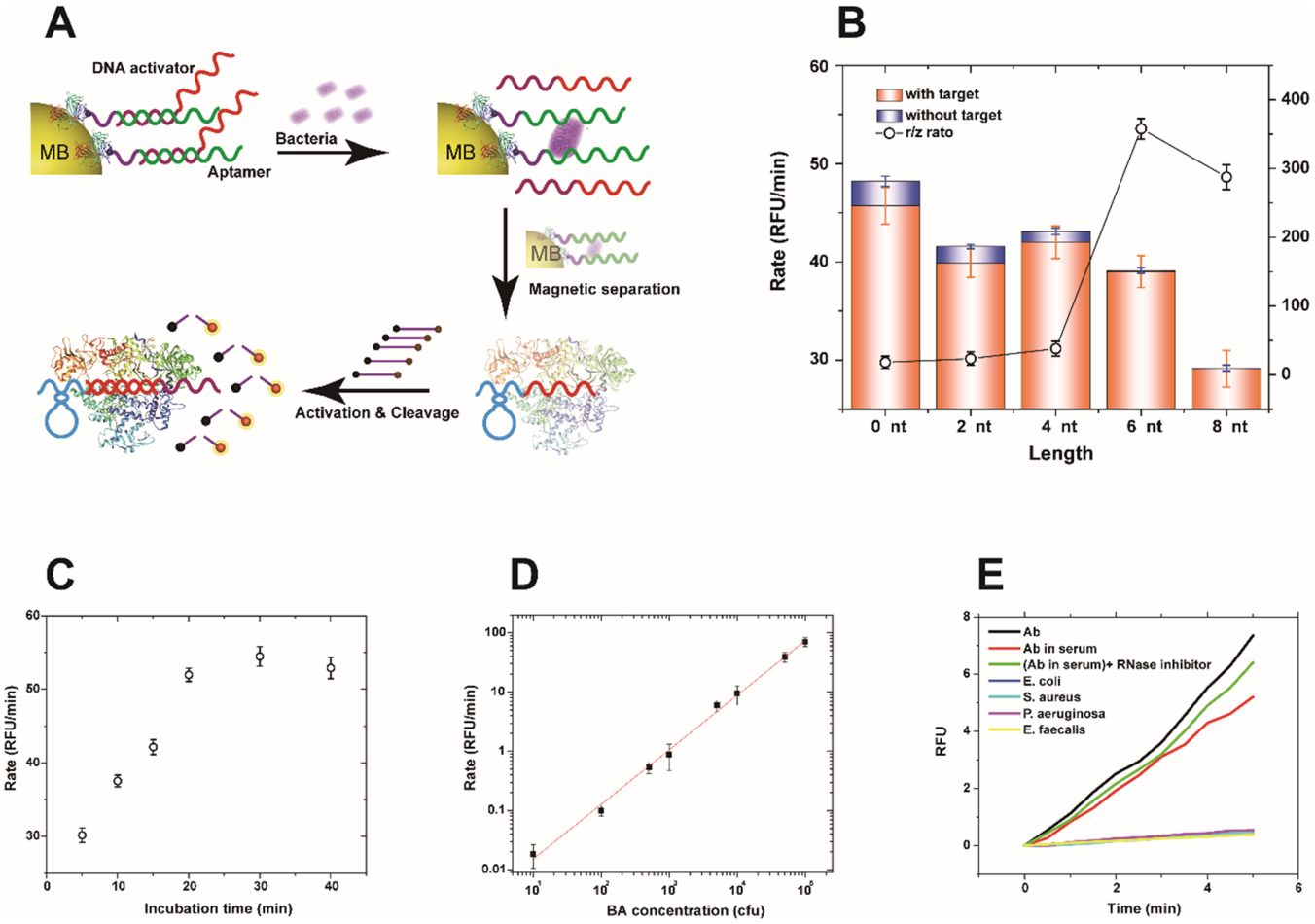


**Figure 3.** CRISPR-Cas12a-based assay for *A. baumannii* (Ab) detection based on Ab-selective aptamer. (A) Schematic illustration of the design of the assay to detect Ab using Ab aptamer. (B) Effect of the c-Ab-Apt length on the $r/z$ ratio of the assay in the presence of Ab. (C) Influence of incubation time on the cleavage rates. (D) Linear fitting of the cleavage rate with Ab in the range of $10-10^5$ CFU/mL. (E) Selectivity of the assay toward interfering bacteria including *E. coli*, *S. aureus*, *P. aeruginosa*, and *E. faecalis* at $10^7$ CFU/mL (the concentration of Ab is 1000 CFU/mL).

subsequent experiment. Freeing the single-stranded nontarget strand (NTS) from the DNA duplex was found to be an essential checkpoint after nuclease activation,[37] while 14 base pairs of the crRNA−DNA heteroduplex at the PAM-proximal end were sufficient to trigger the nuclease activation of Cas12a, and 17 or more base pairs between the crRNA and the TS are needed to fully release the NTS cleavage site to enable quick cleavage. Along with this report, we found that the increase in TS length up to 20 nt resulted in a faster cleavage rate (Figure 1C). With the TS being longer than 20 nt, a declining cleavage rate was observed probably due to slower NTS cleavage site release or the sacrifice of collateral cleavage activity in TS processing. Under optimized conditions, the cleavage rate was titrated with the TS ranging from 0.1 nM to 0.1 $\mu$M (Figure 1D). As depicted in Figure 1E, the cleavage rate was linearly correlated with the TS concentration in the range of 0.1−50 nM, with a detection limit (LOD) down to 1.6 pM (calculated as $3\sigma$/slope, where $\sigma$ is the standard deviation of five blank samples). Besides, when activated by a 5 nM HEX-labeled TS, a time-dependent increase in fluorescence was also observed (Figure 1F). Comparing the relative fluorescence intensity of a 5 nM ssDNA output with that amplified by CRISPR-Cas12a, approximately 160 times signal enhancement is achieved after 15 min of Cas12a processing, which demonstrates the signal amplification power of the CRISPR-Cas12a platform.

**Detection of Lead Ions ($Pb^{2+}$).** To test the ability of the CRISPR-Cas12a platform to detect a broad range of non-DNA targets, we first demonstrate the detection of $Pb^{2+}$ using a well-studied $Pb^{2+}$ DNAzyme GR-5.[38] Widespread $Pb^{2+}$ contamination has posed a great threat to human health, especially on children;[39] therefore, accurate on-site detection and quantification of $Pb^{2+}$ in the surroundings are an important first step to reverse the negative effects.[40] Figure 2A illustrates the overall detection strategy. Specifically, the 3′-end biotinylated substrate strand, which contains the TS sequences at the 5′-end, is attached on the surface of magnetic beads (MBs) through the biotin−streptavidin interaction. Further hybridization with the substrate helps the DNAzyme strand to immobilize on the MBs but could not cause the cleavage of the substrate. Only in the presence of $Pb^{2+}$ the TS sequence-containing part of the substrate releases and remains in the buffer after magnetic separation, which will be used to activate CRISPR-Cas12a subsequently. Although the cleavage speeds of Cas12a activated by an enzymatic product in different time intervals indicate a minimum time of 10 min required to reach the equilibrium (Figure 2C) in the presence of 50 nM $Pb^{2+}$, a longer incubation time of 15 min was applied to ensure complete substrate cleavage in the follow-up experiment. Under this condition, a titration curve using samples with a growing amount of $Pb^{2+}$ (0.01 nM−1.0 $\mu$M) showed a


https://dx.doi.org/10.1021/acssensors.9b02305
ACS Sens. 2020, 5, 970−977

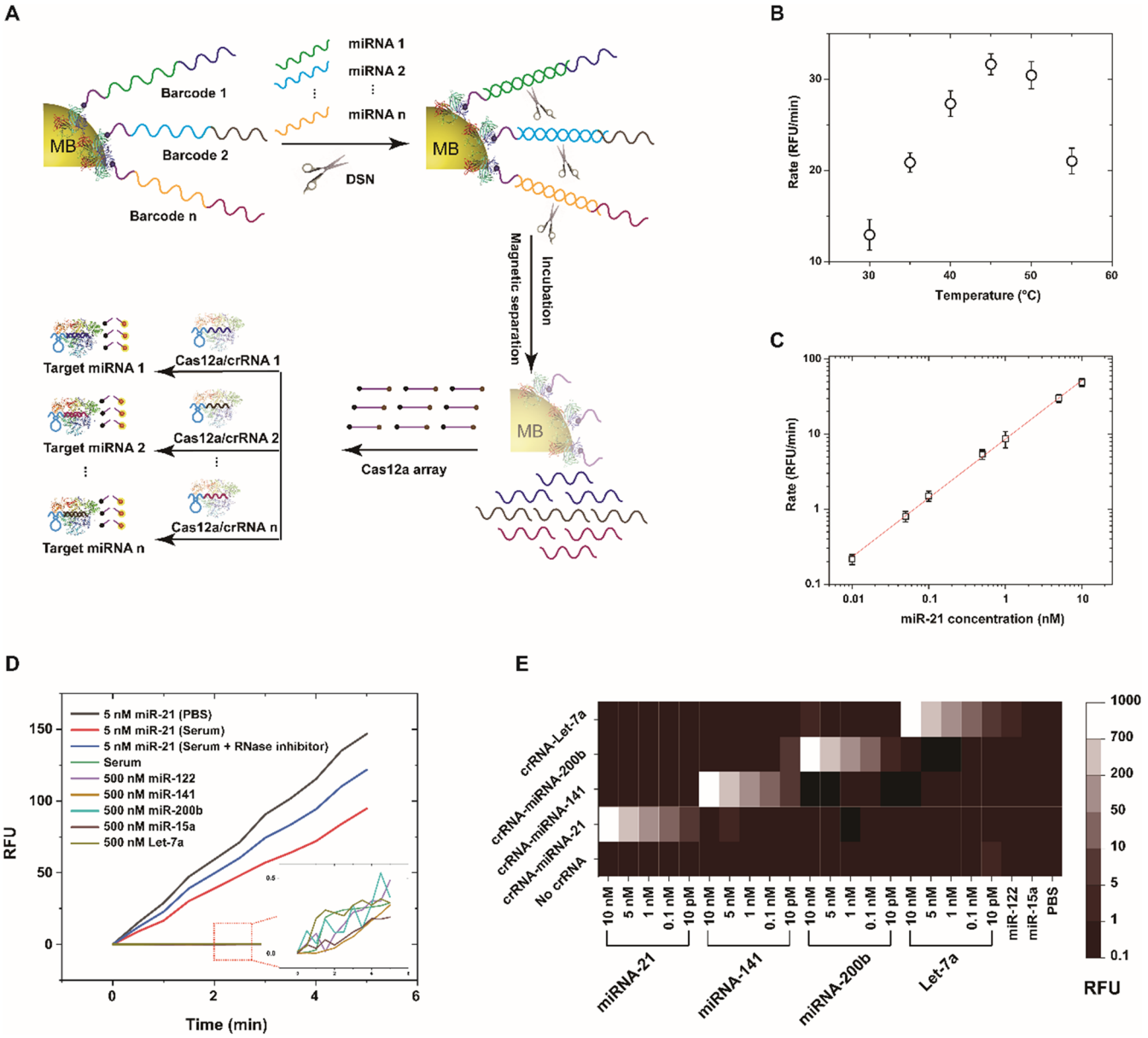


**Figure 4.** CRISPR-Cas12a-based sensor array for multiplexed miRNA analysis based on duplex-specific enzyme and TS tags. (A) Schematic illustration of the design of the sensor array to detect a group of miRNAs simultaneously. (B) Effect of incubation temperature on the cleavage rates in the presence of miR-21. (C) Linear fitting of the cleavage rate with miR-21 concentrations ranging from 10 pM to 10 nM. (D) Selectivity of the assay toward interfering miRNAs including miR-122, miR-141, miR-200b, miR-15a, and Let-7a. (E) Multiplexed detection of miR-21, miR-141, miR-200b, and Let-7a.

concentration-dependent increase in cleavage rates (Figure 2D). The rate increment reaches a plateau at around 10 nM $Pb^{2+}$, indicating the complete cleavage of the substrate at this concentration. When $Pb^{2+}$ higher than 10 nM was used, a slight decline in the cleavage rate was observed, probably due to inhibition of lead ions on the Cas12a activity. In the detection range of ~0.01−10 nM (Figure 2E), the detection limit was estimated to be ~0.053 nM ($3\sigma$/slope), which is four orders of magnitude lower than the Environmental Protection Agency (EPA)-defined maximal contamination level (72 nM) for $Pb^{2+}$ in drinking water and approximately 70 times lower than the $Pb^{2+}$ sensor constructed by direct annealing of fluorophore/quencher-labeled GR-5 DNAzyme and substrates.[38] This is partly due to the fact that the LOD of the latter depends largely on the background signal that originated from the incomplete quenching of the fluorophore by the quencher and the leakage of the substrate from the DNAzyme/substrate duplex, whereas in our design, only the presence of $Pb^{2+}$ causes the release of the cleaved substrate, and the cleavage intermediate would further amplify the fluorescence signal output through the CRISPR-Cas12a platform. In addition to sensitivity, the selectivity of the assay was also investigated in the presence of potential interfering cations containing $K^+$, $Ca^{2+}$, $Zn^{2+}$, $Fe^{3+}$, $Mn^{2+}$, $Cd^{2+}$, $Co^{2+}$, $Ni^{2+}$, and $Cu^{2+}$ in a concentration of 10 $\mu$M (Figure 2B). As expected, no significant fluorescence enhancement was observed except those incubated with 10 nM $Pb^{2+}$ despite the fact that the concentration of interference is a thousand times higher. Therefore, the new assay constructed by the GR-5 DNAzyme and the CRISPR-Cas12a platform has demonstrated an


https://dx.doi.org/10.1021/acssensors.9b02305
ACS Sens. 2020, 5, 970−977

extraordinary specificity toward lead ions when tested against the metal ions individually or as a mixture.

**Detection of *A. baumannii* (Ab).** Given the good performance of the CRISPR-Cas12a platform toward $Pb^{2+}$ ion detection, we further extended our methodology from DNAzyme to aptamer to detect a multivalent target, *A. baumannii*, to test the generality of the construction strategy. This pathogen has emerged as one of the most troublesome organisms for health care institutions globally[41] and is responsible for a majority of increasing recovery of multidrug resistance in the clinic.[42] Similar to the $Pb^{2+}$ DNAzyme assay described above, the Ab aptamer (abbreviated as Ab-Apt) selected previously[43] was immobilized on MBs via streptavidin−biotin binding. The Ab-Apt was then hybridized with a TS sequence-containing strand (c-Ab-Apt) partially complementary to the aptamer, the higher affinity of which toward Ab than the short complementary strand would lead to the release of c-Ab-Apt from the beads when Abs were presented, thus triggering the subsequent CRISPR-Cas12a platform (Figure 3A). First, the complementary sequence of the Ab-Apt was divided into three parts in which a TS tail at the 5′-end was appended, assembled on MBs, and underwent Ab-elicited release to investigate the best hybridization location. The $r/z$ ratio (calculated by dividing the cleavage rate in the presence of Ab by that with the buffer only) in Figure S2 suggests that the location of the complementary strand at the 5′-end is much more vulnerable to discharge than the other two positions in the presence of Abs. To further stabilize the c-Ab-Apt on MBs in the presence of the target, the complementary length was investigated. Figure 3B suggests that fewer complementary sequences resulted in more release of c-Ab-Apt strands (thus, faster cleavage speed) but also led to a higher background signal due to instable hybridization. As a compromise, the c-Ab-Apt were extended with six nucleotides to obtain the highest $r/z$ ratio. By incubating the assembled MBs with an increasing concentration of Ab from 10 to $10^5$ CFU/mL for 30 min (optimized incubation time, Figure 3C), a very good linear fitting curve was obtained between the CRISPR-Cas12a cleavage rate and the Ab concentration (Figure 3D). The theoretical detection limit was estimated down to ∼3 CFU/mL ($3\sigma$/slope), which ultimately approaches the single-cell level. The selectivity of the assay was examined using *Escherichia coli*, *Pseudomonas aeruginosa*, *Enterococcus faecalis*, and *Staphylococcus aureus*. Meanwhile, ∼1000 CFU/mL Ab in PBS buffer initiated the clear cleavage of reporters, and up to $10^7$ CFU/mL of the interfering bacteria did not really activate CRISPR-Cas12a (Figure 3E). Besides, the performance of the assay was also surrogated in human serum. Although ∼30% loss of activity was observed in the untreated serum sample, with over 87% cleavage speed retained when 0.1 unit/mL RNA inhibitor was added into the buffer. Those results collectively demonstrate the potential of the CRISPR-Cas12a-based assay in clinical applications.

**Multiplexed Detection of miRNAs.** One of the most alluring merits of CRISPR-Cas assay is its promise for simultaneous detection of multiple targets.[25] Therefore, we finally explore the multiplexing potential of the CRISPR-Cas12a platform using miRNAs as targets, of which the simultaneous detection offers much more important health-related information than the individuals.[44,45] As illustrated in Figure 4A, biotinylated probe DNA, which is composed of a 20-nt polyA spacer at the 3′-end, a miRNA-specific TS tail at the 5′-end, and a 22-nt recognition region complementary to the target miRNA, was fixed on the MB surface in a similar way mentioned above. Target miRNA can recognize and hybridize with the probe to form DNA/RNA duplexes, which would be targeted by duplex-specific nuclease (DSN) and subsequently cleaved to release the TS tail into the buffer, subsequently initiating the CRISPR-Cas12a collateral cleavage activity. Enzymatic reaction products were added to a preassembled Cas12a/crRNA array to investigate the cleavage rates, which will be correlated in turn to a group of specific miRNAs.

Using miRNA-21 as model miRNA, the reaction condition was optimized to obtain the best assay performance. Temperature is one of the determinant factors for DSN cleavage toward short miRNA/DNA duplexes because a low temperature restricts the nuclease activity, whereas a high temperature impairs miRNA/DNA hybridization. As depicted in Figure 4B, 45 °C is the optimum temperature for the assay as both higher and lower temperatures resulted in reduced enzymatic activity. Besides, an incubation time of ∼60 min is required to achieve the highest cleavage efficiency (Figure S3). Under this condition, the cleavage rates were collected by continuous titration of miRNA-21 in a range from 10 pM to 10 nM. Linear fitting of the concentration of miRNA-21 and the cleavage rate suggested a good correlation therebetween (Figure 4C), and the detection limit was estimated to be 12.6 fM ($3\sigma$/slope), which is better than or at least comparable to a majority of fluorescent miRNA probes.[44,46] The selectivity of the assay was then investigated using a group of potential interferences, including miRNA-122, miRNA-15a, miRNA-141, miRNA-200b, and Let-7a, in a concentration of 500 nM. As shown in Figure 4D, no significant activation of the CRISPR-Cas12a platform was observed even though the concentration of interfering counterparts is 100 times higher than that of the target miRNA-21. Likely due to either inhibition of the enzymatic activity or denaturing of miRNA, the cleavage rate of the miRNA-spiked serum sample is ∼64% of that in PBS. However, like in the Ab detection, the cleavage speed recovers to a higher grade of ∼83% when 0.1 unit/mL RNA inhibitor was applied. Given the good performance of the CRISPR-Cas12a assay toward miRNA, we further extend the methodology to three other miRNA targets including Let-7a, miRNA-141, and miRNA-200b to test the multiplexing capability. As shown in Figure 4E, each CRISPR-Cas12a unit gives significant fluorescence readout only in the presence of both the specific crRNA and the miRNA target. The fluorescence intensity also positively correlates with the concentration of the target miRNA, while interfering miRNAs induce signal strength almost similar to that of blank controls with PBS. Therefore, we conclude that the CRISPR-Cas12a platform can be used to detect a group of miRNAs simultaneously when well-designed barcode probes are provided.

## CONCLUSIONS

In summary, we have demonstrated that CRISPR-Cas12a can be used as a signal amplifier to recognize single-stranded DNA intermediates down to femtomolar concentrations and enhance the fluorescence signal output upon activation. With this good signal amplification power, a fluorescence detection platform is proposed to construct bioassays capable of not only detecting heavy metal ion contamination and bacterial infection with high sensitivity but also realizing multiplexed analysis of miRNA expression profiles in an efficient way. Given the versatility and generality of the CRISPR-Cas12a


https://dx.doi.org/10.1021/acssensors.9b02305
ACS Sens. 2020, 5, 970−977

platform and the rapid evolution of functional nucleotides, it allows the design of a plethora of ultrasensitive biosensors for a wide range of biologically relevant species. More importantly, the CRISPR-Cas12a assays are programmable and promise simultaneous detection of multitargets in high throughput, which would potentially revolutionize analytical science and individualized disease diagnosis to a large extent. Overall, we expect this versatile and efficient biosensor construction strategy to greatly advance the application of CRISPR-Cas-based biodetection platforms in biodiagnosis and provide insights into ultrasensitive bioanalysis.

## ■ ASSOCIATED CONTENT

### Supporting Information

The Supporting Information is available free of charge at https://pubs.acs.org/doi/10.1021/acssensors.9b02305.

Materials and methods used in the study; sequence and modification of oligonucleotides; and supplementary figures of Cas12a cleavage rates with DTT in different concentrations, $r/z$ ratios of the CRISPR-Cas12a assays with c-Ab-apt complementary to the Ab aptamer at different positions, and Cas12a cleavage rates with different incubation times of the DSN mixture with 5 nM miR-21 at 45 °C (PDF)

## ■ AUTHOR INFORMATION


### Corresponding Authors

**Junjie Li** − *Key Laboratory of Laboratory Medical Diagnostics, Ministry of Education, Department of Laboratory Medicine, Chongqing Medical University, Chongqing 400016, China*; Email: lijunjie2006@gmail.com

**Yongcan Guo** − *Department of Laboratory Medicine, Affiliated Traditional Chinese Medicine Hospital of Southwest Medical University, Luzhou 646000, China*; Email: guoyongcan_2004@163.com

**Guoming Xie** − *Key Laboratory of Laboratory Medical Diagnostics, Ministry of Education, Department of Laboratory Medicine, Chongqing Medical University, Chongqing 400016, China*; orcid.org/0000-0002-7497-1964; Email: guomingxie@cqmu.edu.cn

### Authors

**Shuangshuang Yang** − *Key Laboratory of Laboratory Medical Diagnostics, Ministry of Education, Department of Laboratory Medicine, Chongqing Medical University, Chongqing 400016, China*

**Chen Zuo** − *Key Laboratory of Laboratory Medical Diagnostics, Ministry of Education, Department of Laboratory Medicine, Chongqing Medical University, Chongqing 400016, China*

**Ling Dai** − *Key Laboratory of Laboratory Medical Diagnostics, Ministry of Education, Department of Laboratory Medicine, Chongqing Medical University, Chongqing 400016, China*

Complete contact information is available at: https://pubs.acs.org/10.1021/acssensors.9b02305


### Notes

The authors declare no competing financial interest.

## ■ ACKNOWLEDGMENTS

This research was supported by the National Natural Science Foundation of China (no. 81802115), the China Postdoctoral Science Foundation (no. 2018M643425), and Luzhou Municipal People's Government and Southwest Medical University Science and Technology Strategic Cooperation Project (no. 2018LZXNYD-ZK08).

## ■ REFERENCES


(1) Zhang, Y.; Guo, Y.; Xianyu, Y.; Chen, W.; Zhao, Y.; Jiang, X. Nanomaterials for Ultrasensitive Protein Detection. *Adv. Mater.* **2013**, *25*, 3802−3819.

(2) Ellis, D. I.; Brewster, V. L.; Dunn, W. B.; Allwood, J. W.; Golovanov, A. P.; Goodacre, R. Fingerprinting food: current technologies for the detection of food adulteration and contamination. *Chem. Soc. Rev.* **2012**, *41*, 5706−5727.

(3) Ma, W.; Kuang, H.; Xu, L.; Ding, L.; Xu, C.; Wang, L.; Kotov, N. A. Attomolar DNA detection with chiral nanorod assemblies. *Nat. Commun.* **2013**, *4*, 2689.

(4) Courts, C.; Madea, B. Specific micro-RNA signatures for the detection of saliva and blood in forensic body-fluid identification. *J. Forensic Sci.* **2011**, *56*, 1464−1470.

(5) Schwamborn, K.; Caprioli, R. M. Molecular imaging by mass spectrometry — looking beyond classical histology. *Nat. Rev. Cancer* **2010**, *10*, 639−646.

(6) Xu, J.-J.; Zhao, W.-W.; Song, S.; Fan, C.; Chen, H.-Y. Functional nanoprobes for ultrasensitive detection of biomolecules: an update. *Chem. Soc. Rev.* **2014**, *43*, 1601−1611.

(7) Kim, J.; Campbell, A. S.; de Ávila, B. E.-F.; Wang, J. Wearable biosensors for healthcare monitoring. *Nat. Biotechnol.* **2019**, *37*, 389−406.

(8) Lei, J.; Ju, H. Signal amplification using functional nanomaterials for biosensing. *Chem. Soc. Rev.* **2012**, *41*, 2122−2134.

(9) Kishi, J. Y.; Lapan, S. W.; Beliveau, B. J.; West, E. R.; Zhu, A.; Sasaki, H. M.; Saka, S. K.; Wang, Y.; Cepko, C. L.; Yin, P. SABER amplifies FISH: enhanced multiplexed imaging of RNA and DNA in cells and tissues. *Nat. Methods* **2019**, *16*, 533−544.

(10) Shrivastava, S.; Jadon, N.; Jain, R. Next-generation polymer nanocomposite-based electrochemical sensors and biosensors: A review. *TrAC, Trends Anal. Chem.* **2016**, *82*, 55−67.

(11) Baptista, F. R.; Belhout, S. A.; Giordani, S.; Quinn, S. J. Recent developments in carbon nanomaterial sensors. *Chem. Soc. Rev.* **2015**, *44*, 4433−4453.

(12) Dang, S.; Zhu, Q.-L.; Xu, Q. Nanomaterials derived from metal−organic frameworks. *Nat. Rev. Mater.* **2018**, *3*, 17075.

(13) Nam, J.-M.; Thaxton, C. S.; Mirkin, C. A. Nanoparticle-based bio-bar codes for the ultrasensitive detection of proteins. *Science* **2003**, *301*, 1884−1886.

(14) Hill, H. D.; Mirkin, C. A. The bio-barcode assay for the detection of protein and nucleic acid targets using DTT-induced ligand exchange. *Nat. Protoc.* **2006**, *1*, 324−336.

(15) Maynard, A. D.; Aitken, R. J. 'Safe handling of nanotechnology' ten years on. *Nat. Nanotechnol.* **2016**, *11*, 998.

(16) Lin, L. C.-W.; Chattopadhyay, S.; Lin, J.-C.; Hu, C.-M. J. Advances and opportunities in nanoparticle-and nanomaterial-based vaccines against bacterial infections. *Adv. Healthcare Mater.* **2018**, *7*, 1701395.

(17) Bienko, M.; Crosetto, N.; Teytelman, L.; Klemm, S.; Itzkovitz, S.; Van Oudenaarden, A. A versatile genome-scale PCR-based pipeline for high-definition DNA FISH. *Nat. Methods* **2013**, *10*, 122.

(18) Kazane, S. A.; Sok, D.; Cho, E. H.; Uson, M. L.; Kuhn, P.; Schultz, P. G.; Smider, V. V. Site-specific DNA-antibody conjugates for specific and sensitive immuno-PCR. *Proc. Natl. Acad. Sci. U. S. A.* **2012**, *109*, 3731−3736.

(19) Shlyapnikov, Y. M.; Malakhova, E. A.; Shlyapnikova, E. A. Rapid Amplification-Free Microarray-Based Ultrasensitive Detection of DNA. *Anal. Chem.* **2019**, *91*, 11209−11214.

(20) Cong, L.; Ran, F. A.; Cox, D.; Lin, S.; Barretto, R.; Habib, N.; Hsu, P. D.; Wu, X.; Jiang, W.; Marraffini, L. A.; Zhang, F. Multiplex genome engineering using CRISPR/Cas systems. *Science* **2013**, *339*, 819−823.

(21) Horvath, P.; Barrangou, R. CRISPR/Cas, the immune system of bacteria and archaea. *Science* **2010**, *327*, 167−170.
(22) Sander, J. D.; Joung, J. K. CRISPR-Cas systems for editing, regulating and targeting genomes. *Nat. Biotechnol.* **2014**, *32*, 347.
(23) Makarova, K. S.; Haft, D. H.; Barrangou, R.; Brouns, S. J. J.; Charpentier, E.; Horvath, P.; Moineau, S.; Mojica, F. J. M.; Wolf, Y. I.; Yakunin, A. F.; van der Oost, J.; Koonin, E. V. Evolution and classification of the CRISPR−Cas systems. *Nat. Rev. Microbiol.* **2011**, *9*, 467.
(24) Gootenberg, J. S.; Abudayyeh, O. O.; Lee, J. W.; Essletzbichler, P.; Dy, A. J.; Joung, J.; Verdine, V.; Donghia, N.; Daringer, N. M.; Freije, C. A.; Myhrvold, C.; Bhattacharyya, R. P.; Livny, J.; Regev, A.; Koonin, E. V.; Hung, D. T.; Sabeti, P. C.; Collins, J. J.; Zhang, F. Nucleic acid detection with CRISPR-Cas13a/C2c2. *Science* **2017**, *356*, 438−442.
(25) Gootenberg, J. S.; Abudayyeh, O. O.; Kellner, M. J.; Joung, J.; Collins, J. J.; Zhang, F. Multiplexed and portable nucleic acid detection platform with Cas13, Cas12a, and Csm6. *Science* **2018**, *360*, 439−444.
(26) Wang, T.; Liu, Y.; Sun, H.-H.; Yin, B.-C.; Ye, B.-C. An RNA-Guided Cas9 Nickase-Based Method for Universal Isothermal DNA Amplification. *Angew. Chem., Int. Ed.* **2019**, *58*, 5382−5386.
(27) Chen, J. S.; Ma, E.; Harrington, L. B.; Da Costa, M.; Tian, X.; Palefsky, J. M.; Doudna, J. A. CRISPR-Cas12a target binding unleashes indiscriminate single-stranded DNase activity. *Science* **2018**, *360*, 436−439.
(28) Li, S.-Y.; Cheng, Q.-X.; Liu, J.-K.; Nie, X.-Q.; Zhao, G.-P.; Wang, J. CRISPR-Cas12a has both cis- and trans-cleavage activities on single-stranded DNA. *Cell Res.* **2018**, *28*, 491−493.
(29) Li, S.-Y.; Cheng, Q.-X.; Wang, J.-M.; Li, X.-Y.; Zhang, Z.-L.; Gao, S.; Cao, R.-B.; Zhao, G.-P.; Wang, J. CRISPR-Cas12a-assisted nucleic acid detection. *Cell Discovery* **2018**, *4*, 20.
(30) Qian, C.; Wang, R.; Wu, H.; Zhang, F.; Wu, J.; Wang, L. Uracil-Mediated New Photospacer-Adjacent Motif of Cas12a To Realize Visualized DNA Detection at the Single-Copy Level Free from Contamination. *Anal. Chem.* **2019**, *91*, 11362−11366.
(31) Hajian, R.; Balderston, S.; Tran, T.; DeBoer, T.; Etienne, J.; Sandhu, M.; Wauford, N. A.; Chung, J.-Y.; Nokes, J.; Athaiya, M.; Paredes, J.; Peytavi, R.; Goldsmith, B.; Murthy, N.; Conboy, I. M.; Aran, K. Detection of unamplified target genes via CRISPR−Cas9 immobilized on a graphene field-effect transistor. *Nat. Biomed. Eng.* **2019**, *3*, 427−437.
(32) Liang, M.; Li, Z.; Wang, W.; Liu, J.; Liu, L.; Zhu, G.; Karthik, L.; Wang, M.; Wang, K.-F.; Wang, Z.; Yu, J.; Shuai, Y.; Yu, J.; Zhang, L.; Yang, Z.; Li, C.; Zhang, Q.; Shi, T.; Zhou, L.; Xie, F.; Dai, H.; Liu, X.; Zhang, J.; Liu, G.; Zhou, Y.; Zhang, B.; Liu, C.; Li, S.; Xia, X.; Tong, Y.; Liu, Y.; Alterovitz, G.; Tan, G.-Y.; Zhang, L.-X. A CRISPR-Cas12a-derived biosensing platform for the highly sensitive detection of diverse small molecules. *Nat. Commun.* **2019**, *10*, 3672.
(33) English, M. A.; Soenksen, L. R.; Gayet, R. V.; de Puig, H.; Angenent-Mari, N. M.; Mao, A. S.; Nguyen, P. Q.; Collins, J. J. Programmable CRISPR-responsive smart materials. *Science* **2019**, *365*, 780−785.
(34) Jeon, Y.; Choi, Y. H.; Jang, Y.; Yu, J.; Goo, J.; Lee, G.; Jeong, Y. K.; Lee, S. H.; Kim, I.-S.; Kim, J.-S.; Jeong, C.; Lee, S.; Bae, S. Direct observation of DNA target searching and cleavage by CRISPR-Cas12a. *Nat. Commun.* **2018**, *9*, 2777.
(35) Singh, D.; Mallon, J.; Poddar, A.; Wang, Y.; Tippana, R.; Yang, O.; Bailey, S.; Ha, T. Real-time observation of DNA target interrogation and product release by the RNA-guided endonuclease CRISPR Cpf1 (Cas12a). *Proc. Natl. Acad. Sci. U. S. A.* **2018**, *115*, 5444−5449.
(36) Shaman, J. A.; Prisztoka, R.; Ward, W. S. Topoisomerase IIB and an extracellular nuclease interact to digest sperm DNA in an apoptotic-like manner. *Biol. Reprod.* **2006**, *75*, 741−748.
(37) Zhang, L.; Sun, R.; Yang, M.; Peng, S.; Cheng, Y.; Chen, C. Conformational Dynamics and Cleavage Sites of Cas12a Are Modulated by Complementarity between crRNA and DNA. *iScience* **2019**, *19*, 492−503.
(38) Lan, T.; Furuya, K.; Lu, Y. A highly selective lead sensor based on a classic lead DNAzyme. *Chem. Commun.* **2010**, *46*, 3896−3898.
(39) Magyar, J. S.; Weng, T.-C.; Stern, C. M.; Dye, D. F.; Rous, B. W.; Payne, J. C.; Bridgewater, B. M.; Mijovilovich, A.; Parkin, G.; Zaleski, J. M.; Penner-Hahn, J. E.; Godwin, H. A. Reexamination of Lead(II) Coordination Preferences in Sulfur-Rich Sites: Implications for a Critical Mechanism of Lead Poisoning. *J. Am. Chem. Soc.* **2005**, *127*, 9495−9505.
(40) Xiang, Y.; Tong, A.; Lu, Y. Abasic Site-Containing DNAzyme and Aptamer for Label-Free Fluorescent Detection of $Pb^{2+}$ and Adenosine with High Sensitivity, Selectivity, and Tunable Dynamic Range. *J. Am. Chem. Soc.* **2009**, *131*, 15352−15357.
(41) McConnell, M. J.; Actis, L.; Pachón, J. Acinetobacter baumannii: human infections, factors contributing to pathogenesis and animal models. *FEMS Microbiol. Rev.* **2013**, *37*, 130−155.
(42) Dijkshoorn, L.; Nemec, A.; Seifert, H. An increasing threat in hospitals: multidrug-resistant Acinetobacter baumannii. *Nat. Rev. Microbiol.* **2007**, *5*, 939−951.
(43) Rasoulinejad, S.; Gargari, S. L. M. Aptamer-nanobody based ELASA for specific detection of Acinetobacter baumannii isolates. *J. Biotechnol.* **2016**, *231*, 46−54.
(44) Li, J.; Tan, S.; Kooger, R.; Zhang, C.; Zhang, Y. MicroRNAs as novel biological targets for detection and regulation. *Chem. Soc. Rev.* **2014**, *43*, 506−517.
(45) Dong, H.; Lei, J.; Ding, L.; Wen, Y.; Ju, H.; Zhang, X. MicroRNA: function, detection, and bioanalysis. *Chem. Rev.* **2013**, *113*, 6207−6233.
(46) Jin, Z.; Geißler, D.; Qiu, X.; Wegner, K. D.; Hildebrandt, N. A Rapid, Amplification-Free, and Sensitive Diagnostic Assay for Single-Step Multiplexed Fluorescence Detection of MicroRNA. *Angew. Chem., Int. Ed.* **2015**, *54*, 10024−10029.


https://dx.doi.org/10.1021/acssensors.9b02305
*ACS Sens.* 2020, 5, 970−977